Coregulation of vascular tube stabilization by endothelial cell TIMP-2 and pericyte TIMP-3

W. Brian Saunders,[1] Brenda L. Bohnsack,[4] Jennifer B. Faske,[1] Nicholas J. Anthis,[1] Kayla J. Bayless,[1] Karen K. Hirschi,[4] and George E. Davis[1,2,3]

[1]Department of Pathology and Laboratory Medicine, Texas A&M University System Health Science Center, College Station, TX 77843
[2]Department of Medical Pharmacology and Physiology and [3]Department of Pathology and Anatomical Sciences, School of Medicine, Christopher S. Bond Life Sciences Center and Dalton Cardiovascular Research Center, University of Missouri-Columbia, Columbia, MO 65212
[4]Center for Cell and Gene Therapy, Baylor College of Medicine, Houston, TX 77030

The endothelial cell (EC)–derived tissue inhibitor of metalloproteinase-2 (TIMP-2) and pericyte-derived TIMP-3 are shown to coregulate human capillary tube stabilization following EC–pericyte interactions through a combined ability to block EC tube morphogenesis and regression in three-dimensional collagen matrices. EC–pericyte interactions strongly induce TIMP-3 expression by pericytes, whereas ECs produce TIMP-2 in EC–pericyte cocultures. Using small interfering RNA technology, the suppression of EC TIMP-2 and pericyte TIMP-3 expression leads to capillary tube regression in these cocultures in a matrix metalloproteinase-1 (MMP-1)–, MMP-10–, and ADAM-15 (a disintegrin and metalloproteinase-15)–dependent manner. Furthermore, we show that EC tube morphogenesis (lumen formation and invasion) is primarily controlled by the TIMP-2 and -3 target membrane type (MT) 1 MMP. Additional targets of these inhibitors include MT2-MMP and ADAM-15, which also regulate EC invasion. Mutagenesis experiments reveal that TIMP-3 requires its proteinase inhibitory function to induce tube stabilization. Overall, these data reveal a novel role for both TIMP-2 and -3 in the pericyte-induced stabilization of newly formed vascular networks that are predisposed to undergo regression and reveal specific molecular targets of the inhibitors regulating these events.

Introduction

During angiogenesis, a complex coordination of cues from cytokines, growth factors, proteinases, and integrins mediate cellular changes to control the processes of sprouting, lumen formation, and proliferation (Davis et al., 2002; Carmeliet, 2005; Davis and Senger, 2005). Once networks of endothelial cell (EC)–lined tubes are formed, the stabilization of these structures is regulated by support cells such as pericytes (Orlidge and D'Amore, 1987; Jain, 2003; von Tell et al., 2006). In PDGF-B and -β receptor knockout mice, the lack of pericyte recruitment results in vascular instability and embryonic lethality (Lindahl et al., 1997; Hirschi et al., 1998; Hellstrom et al., 1999, 2001; Jain, 2003). A molecular understanding of how pericyte–EC interactions lead to EC tube stability is not well understood

and is an emerging field in vascular biology (Jain, 2003; Davis and Senger, 2005; von Tell et al., 2006).

Matrix metalloproteinases (MMPs) regulate many biological processes, including ECM degradation, proteolysis of cell surface proteins, proteinase zymogen activation, liberation of growth factors, and regulation of tissue morphogenesis (Nagase and Woessner, 1999; Davis et al., 2002; Kheradmand and Werb, 2002), which includes vascularization (Pepper, 2001; Davis et al., 2002). Membrane-type (MT) MMPs but not soluble MMPs have been shown to play a critical role in cellular invasion through 3D matrices by degrading ECM proteins at the cell surface–ECM interface while maintaining the integrity of the surrounding ECM scaffold (Hotary et al., 2000, 2002; Lafleur et al., 2002; Bayless and Davis, 2003; Chun et al., 2004). MMPs are controlled by various inhibitors, including tissue inhibitor of metalloproteinases-1–4 (TIMPs-1–4; Baker et al., 2002). TIMPs have been shown to regulate angiogenesis, wound repair, and tumor metastasis (Anand-Apte et al., 1997; Lafleur et al., 2001; Spurbeck et al., 2002; Seo et al., 2003; Stetler-Stevenson and Seo, 2005), and a balance of MMPs and TIMPs appears to be critical during these events. Interestingly, MMPs appear to

contribute to tissue regression in the mammary gland (Green and Lund, 2005), vasculature (Davis et al., 2001; Saunders et al., 2005; Davis and Saunders, 2006), and during the menstrual cycle (Curry and Osteen, 2003). In this study, we present the novel concept that EC-derived TIMP-2 and pericyte-derived TIMP-3 coregulate capillary tube stabilization by the inhibition of key EC targets such as MT1-MMP, ADAM-15 (a disintegrin and metalloproteinase-15), MMP-1, and MMP-10, which normally control EC tube formation and/or regression.

Results

TIMP-2 and -3 markedly inhibit EC invasion and tubular morphogenesis events in 3D collagen matrices

Using an in vitro model of angiogenic sprouting, human ECs invade ~500 μm into 3D collagen matrices over a 48-h period (Fig. 1 A). This invasion response is completely inhibited by TIMP-2 and -3 (Fig. 1, A and B) but not by TIMP-1. Although control and TIMP-1–treated invading ECs form lumenal structures, no lumen formation is seen from TIMP-2– or -3–treated invading ECs (Fig. 1 B). Similar results using ECs transfected

with lentiviral vectors expressing control GFP, TIMP-1, or TIMP-3 were observed (Fig. S1 A, available at http://www.jcb.org/cgi/content/full/jcb.200603176/DC1).

Time-lapse videos were performed with ECs suspended as individual cells within collagen matrices (vasculogenesis-like assay; Davis et al., 2002) over a 48-h period and treated with TIMP-1, -2, or -3 versus the control (Videos 1–4, available at http://www.jcb.org/cgi/content/full/jcb.200603176/DC1). Photographs from these videos are shown at 48 h of culture (Fig. 1 C). ECs treated with TIMP-2 and -3 fail to form tubes (i.e., no lumen structures observed) and instead send out fine processes over this time course (Fig. 1 C, arrowheads; and Videos 1–4). Addition of the chemical MMP inhibitor GM6001 shows essentially identical results, suggesting that these effects are likely the result of proteinase inhibition (Video 5). In contrast, obvious lumenal and tube structures are observed in the control and TIMP-1–treated cultures (Fig. 1 C). Quantitation of the sprouting assay as well as quantitation of the vasculogenesis assay reveals marked blockade of invasion and lumen formation by both TIMP-2 and -3 (Fig. 1 D). These results demonstrate that both TIMP-2 and -3 completely inhibit EC invasion and lumen formation (perhaps indicating a common molecular target), whereas TIMP-1 has no effect.
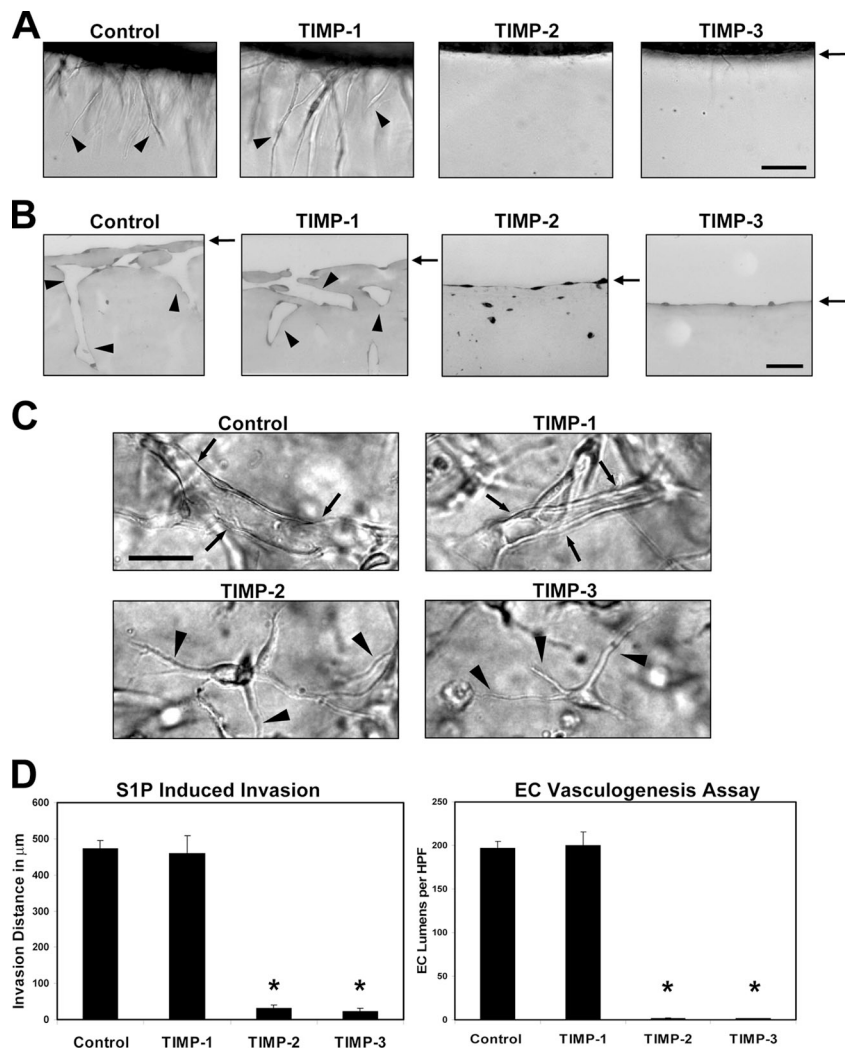

Figure 1. **EC invasion and tubular morphogenesis in 3D collagen matrices are inhibited by TIMP-2 and -3.** (A) ECs were seeded onto collagen matrices and stimulated to invade for 48 h in response to 1 μM S1P in the absence (control) or presence of 5 μg/ml TIMP-1, -2, or -3. Arrows indicate the EC monolayer; arrowheads point to the invading EC sprouts. Bar, 100 μm. (B) Plastic sections of these cultures are shown to illustrate the presence (control; TIMP-1) or absence (TIMP-2 and -3) of EC lumenal structures (arrowheads). Arrows indicate the EC monolayer; arrowheads point to EC lumens. Bar, 40 μm. (C) ECs were suspended within collagen matrices and allowed to undergo morphogenesis and tube network formation for 48 h in the absence (control) or presence of 5 μg/ml TIMP-1, -2, or -3 using time-lapse microscopy. Arrows point to multicellular EC tube networks; arrowheads indicate fine processes. Bar, 50 μm. (D) Graphs show the mean invasion distance in micrometers (left) or the total number of ECs forming lumens (right) ± SD (error bars) using time-lapse images at 48 h. *, P < 0.01 for TIMP-2– or -3–treated ECs compared with controls. HPF, high-powered field.

TIMP-3 markedly blocks vasculogenesis and angiogenesis in mouse embryo cultures

To determine the ability of TIMP-3 to affect vessel formation in vivo, mouse embryo cultures were established from embryonic day (E) 7.5 to E9.5 in the presence of TIMP-1, TIMP-3, GM6001, and DMSO control (Fig. 2 A). Untreated, DMSO, and TIMP-1–treated cultures were photographed live at 48 h and exhibited the remodeling of capillary networks, large vitelline vessels at the origin in the embryo, and large vessels leading to capillaries. The large vitelline vessels (Fig. 2 A, insets) along with capillary networks stained positively for vascular endothelial (VE) cadherin. TIMP-3– and GM6001–treated embryos lacked vitelline vessels, exhibited an immature capillary plexus, and failed to turn. No large vessel structures were formed in GM6001– (unpublished data) or TIMP-3–treated explants as compared with the untreated or TIMP-1–treated explants. These data indicate that TIMP-3 treatment blocked the assembly of vascular structures in vivo, which directly correlated with our in vitro findings.

TIMP-3 is expressed by perivascular mesenchymal cells and the visceral endoderm during early vascular development

RT-PCR analysis of embryonic region (E6.5 and E7.5), extraembryonic region (6.5× and 7.5×), and yolk sac (8.5 and 9.5 d) tissues during vascular development revealed that TIMP-3 was expressed abundantly in both embryonic and extraembryonic tissue as well as by the yolk sac at the time points indicated (Fig. 2 B). TIMP-3 showed increased expression up to E8.5,

whereas TIMP-1 expression decreased over this time period. Immunofluorescence imaging of visceral endoderm and mesoderm sections of yolk sac at E8.5 and E9.5 revealed the colocalization of TIMP-3 with angiopoietin-1 in perivascular mesenchymal cells (pericyte and vascular smooth muscle precursors), which surround the early vascular tubes (Fig. 2 C). Also, strong staining for TIMP-3 was observed in the visceral endoderm, an important supporting structure that controls development of the early vasculature (Bohnsack et al., 2004). These staining distributions were confirmed by in situ hybridization (unpublished data). Thus, the visceral endoderm and mesenchyme surrounding EC tubes (stained with VE-cadherin; Fig. 2 C) in the mesoderm may serve to control and stabilize EC tubular morphogenesis by delivering TIMP-3 to newly formed vascular tubes.

TIMP-3 stabilizes preexisting capillary tube networks by blocking tube formation and MMP-1–dependent tube regression

Because TIMP-3 completely inhibits EC tube morphogenesis, we asked whether TIMP-3 could induce the collapse and regression of preexisting networks of capillary tubes. A previous study revealed that $\alpha2$-integrin–blocking antibodies interfere with the formation of tubes but also cause the rapid collapse (within several hours) of previously formed tube networks (Davis et al., 2001). EC cultures were treated at different times with TIMP-1, -3, or blocking antibodies directed to the $\alpha2$- and $\alpha5$-integrin subunits (Fig. S2, available at http://www.jcb.org/cgi/content/full/jcb.200603176/DC1). The treatment of EC cultures from 0–8 or 0–24 h with $\alpha2$-integrin–blocking
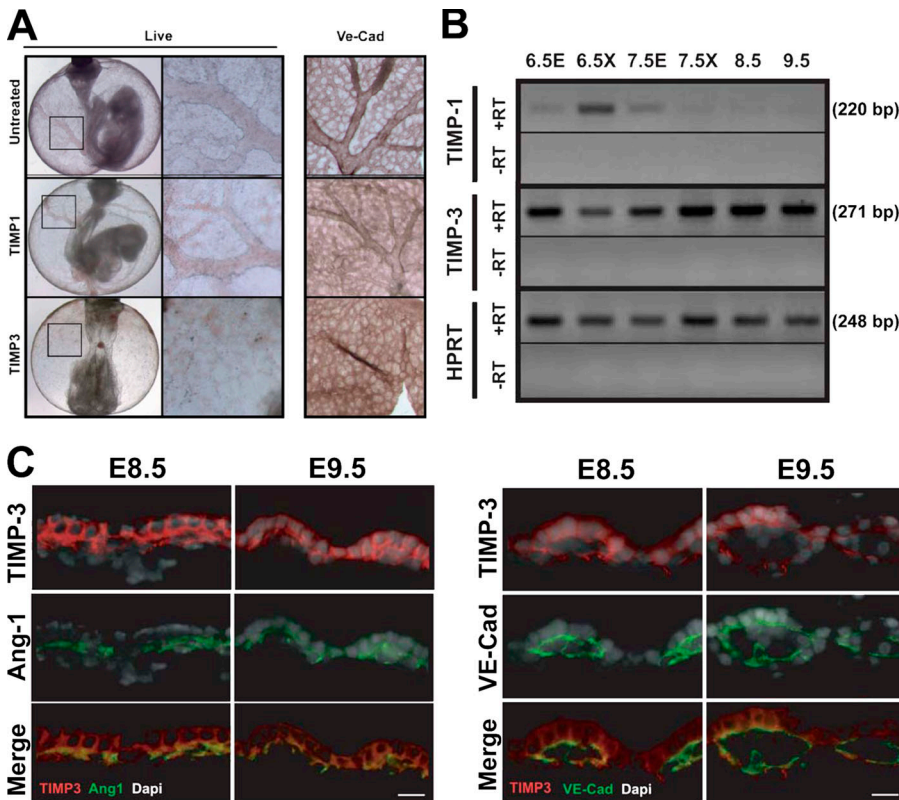

Figure 2. **MT metalloproteinases are required for the remodeling of vascular networks in vivo during mouse vascular development, and TIMP-3 is expressed by perivascular mesenchyme.** (A) E7.5 cultures were established as described previously (Bohnsack et al., 2004) and, in addition, were incubated in the presence of 5 μg/ml TIMP-1 or -3. Cultures were photographed live (left two panels) or were immunostained (right) after 48 h for VE-cadherin expression. Magnified live images from the boxed areas are shown in the adjacent panels for each treatment condition. (B) RT-PCR analysis was performed on extraembryonic (X) and embryonic tissue (E) at the days indicated using primers specific for TIMP-1, -3, and control. (C) Tissue sections at the indicated times were stained with antibodies directed to TIMP-3, VE-cadherin, and angiopoietin-1 (Ang-1). Bars, 100 μm.

antibodies or TIMP-3 strongly inhibited intracellular vacuole and lumen formation (Fig. S2, A and B). TIMP-1 addition or blocking antibodies directed to the α5-integrin subunit had no effect and were identical to the control. The addition of these agents to preestablished EC networks (48 h) revealed that although α2-integrin–blocking antibodies completely collapsed lumenal structures and tubular networks, TIMP-3 did not have this effect (Fig. S2 C). From these data, we hypothesized that TIMP-3 may serve as a stabilizing signal by preventing further morphogenic events and blocking the natural tendency of EC tubes to regress. A time-lapse experiment shown in Fig. S3 supports this conclusion in that TIMP-3 addition to preformed tubes does not cause collapse but retards further morphogenic progression, whereas TIMP-1 addition had no effect on either process.

We also tested the ability of TIMP-3 to block proteinase-mediated regression of endothelial networks. We used a previously established model for EC network regression and collagen gel contraction (Davis et al., 2001; Saunders et al., 2005) in which ECs were allowed to assemble into tube networks for 24 h before plasminogen (Plg) addition to activate pro–MMP-1 and -10. Cultures were either left untreated (control) or were treated with TIMP-1 or -3. After 48 h, cultures were fixed, and the percentage of collagen gel contraction was quantitated (collagen gel contraction represents the end stage of capillary tubular network collapse after proteolysis of the collagen gel matrix scaffold). These data are shown in Fig. S2 D, and they support the concept that TIMP-3 functions to stabilize and prevent the regression of EC networks. TIMP-1 also inhibits regression events that are regulated by MMP-1 and -10, which is consistent with our previous observations (Davis et al., 2001; Saunders et al., 2005). TIMP-2 and GM6001 show essentially identical effects compared with TIMP-3 in these latter assays (unpublished data).

Marked production of TIMP-3 by pericytes and regulation of pericyte TIMP-3 production by ECs in 3D collagen matrices

Pericytes are known to stabilize the developing or wound vasculature (von Tell et al., 2006). We hypothesized that perhaps pericytes deliver TIMP-3 to EC tubes to stabilize them. To evaluate TIMP-3 production by vascular cells, including EC, bovine retinal pericytes (BRPs), and coronary artery smooth muscle cells (CASMCs), cells were cultured on plastic substrates and treated with or without TGF-β for 24 h (Fig. S1 B). Western blot analyses of cell lysates revealed that TIMP-3 was not produced by ECs. However, marked production of TIMP-3 was observed from pericytes and to a lesser degree by CASMCs.

Because pericytes appear to be a strong source of TIMP-3, 3D cocultures were established with ECs and pericytes at varying pericyte/EC ratios using constant levels of ECs (Fig. 3 A). In addition, we performed the reverse experiment whereby pericytes were added at a constant level and ECs were added at varying levels (Fig. 3 B). As shown in Fig. 3 (A and B), increasing the levels of pericytes in the presence of constant ECs or increasing the levels of ECs with constant pericytes leads to a strong increase in TIMP-3 production. Interestingly, TIMP-3 is strongly produced by pericytes on plastic dishes (Fig. S1 B), but this production markedly decreases when they are cultured alone in 3D collagen matrices (Fig. 3 B). Importantly, the coculture of ECs with pericytes strongly induces TIMP-3 production by pericytes (Fig. 3, A and B). In contrast, it is clear that ECs are by far the predominant source of TIMP-2, TIMP-1, and PAI-1 in this 3D model. Little production of these factors is seen from pericytes alone, whereas the strong production of each of these factors is observed with ECs alone. To evaluate this conclusion further, siRNA suppression experiments were performed using both ECs and pericytes in 3D culture to assess which cell type is producing each proteinase inhibitor. As shown in Fig. 3,
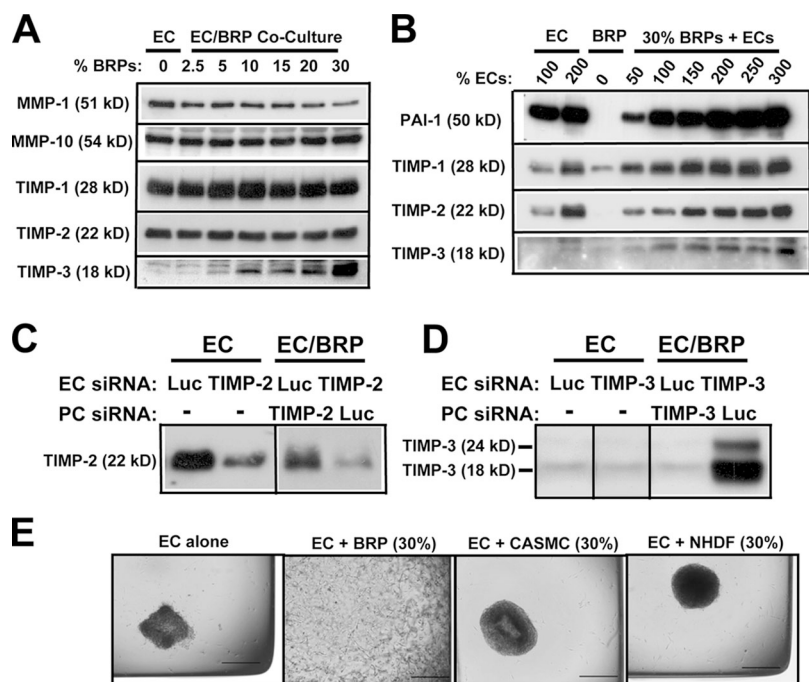
Figure 3. **Coculture of ECs with BRPs results in a marked induction of pericyte-derived TIMP-3 and a decreased production of EC-derived MMP-1.** (A) ECs were suspended in 3D collagen matrices and cultured alone or in the presence of varying amounts of BRPs relative to EC number for 48 h before the collection of conditioned media or preparation of cell extracts. (B) Varying concentrations of ECs (relative to 100% EC culture) were cocultured with 3×10^5 cells/ml BRPs or were cultured alone. Western blots for the indicated antigens were performed. (C) ECs treated with TIMP-2 siRNA were cocultured with BRPs treated with luciferase control siRNA (Luc) and vice versa as shown. PC, pericyte. (D) ECs transfected with TIMP-3 siRNA were cocultured with BRPs transfected with Luc siRNA and vice versa as shown. (C and D) Western blots are shown to determine the indicated TIMP expression after treatment. (E) ECs were cultured alone or in the presence of 30% BRPs (relative to 100% ECs), CASMCs, or normal human dermal fibroblasts (NHDFs) in the presence of 1 μg/ml plasmin for 48 h. Unstained cultures were photographed to assess the extent of regression and gel contraction. Bars, 500 μm.

siRNAs directed to these proteins show that ECs are the predominant source of TIMP-2, TIMP-1, and PAI-1, whereas pericytes are the source of TIMP-3. Thus, it appears that TIMP-3 production is markedly regulated by EC–pericyte interactions, whereas the other proteinase inhibitors do not appear to be altered. Interestingly, pro–MMP-1 levels, which control capillary tube regression, are progressively decreased with increasing levels of pericytes in the cocultures (Fig. 3 A). In contrast, pro–MMP-10 levels do not change under the same conditions.

Pericytes completely block MMP-1– and -10–dependent capillary tube regression events leading to capillary tube stabilization

To address whether pericytes are able to contribute to capillary tube stabilization through the blockade of MMP-1– and -10–dependent tube regression, cocultures were prepared, and quantitative analysis of tube regression over time was examined.
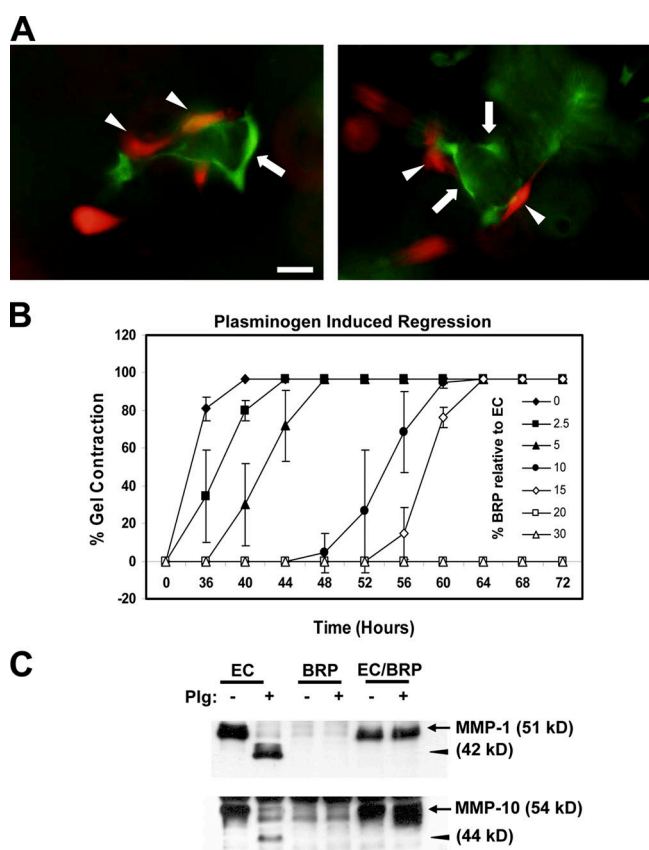

A

B

Plasminogen Induced Regression

C

Figure 4. **Pericytes markedly block EC tube regression via the inhibition of MMP-1 and -10.** (A) EC or BRP stable cell lines expressing GFP or mRFP, respectively, were cocultured with 30% BRPs relative to ECs for 72 h before fluorescence photography. Pericytes (arrowheads) are shown associating with EC-lined tubes (arrows). Bar, 50 μm. (B) ECs were suspended in 3D collagen matrices in the presence of an increasing concentration of BRPs (shown as the percentage relative to ECs). Cultures were supplied with standard media containing 2 μg/ml Plg. Cultures were monitored every 4 h for EC tubular network collapse and collagen gel contraction. Data are reported as the mean percent collagen gel contraction ± SD (error bars) at the indicated times ($n = 8$). (C) At 72 h, conditioned media were collected and analyzed for MMP-1 and -10 expression and activation via Western blotting. Arrows indicate proenzymes; arrowheads point to activated enzymes.

To illustrate the coculture system, GFP-labeled ECs were cocultured with mRFP-labeled (Campbell et al., 2002) pericytes, which clearly shows the ability of pericytes to associate with developing EC tubes (Fig. 4 A). As shown in Fig. 4 B, the addition of pericytes induced a strong delay in regression until the addition of 20 or 30% pericytes relative to ECs where tube regression is completely inhibited. To examine whether the tube regression event correlates with pro–MMP-1 or -10 activation, Western blots were performed (Fig. 4 B). The addition of 30% pericytes completely blocks MMP-1 and -10 activation in response to Plg addition, indicating that proteinase inhibition is the most likely mechanism by which pericytes interfere with the capillary tube regression response (Fig. 4 B). To address whether pericytes were unique in their ability to block EC tube regression, 30% human fibroblasts or CASMCs were added, and neither cell type was able to block the regression response like the pericytes at this cell/EC percentage (Fig. 3 E).

EC-derived TIMP-2 and pericyte-derived TIMP-3 prevent capillary tube regression events (leading to tube stabilization) in EC–pericyte cocultures

To address the role of the different TIMPs and PAI-1 in this coculture model of pericyte-induced capillary tube stabilization, siRNA suppression was used. As shown in Fig. 5, siRNA suppression of specific TIMPs in ECs versus pericytes was observed relative to an actin control. In this experiment, ECs were treated with luciferase control, TIMP-1, or -2 siRNAs, whereas pericytes were treated with luciferase control or TIMP-3 siRNA. The different cell types were mixed in different combinations and were cultured in 3D collagen matrices at two pericyte/EC ratios of 30 or 50% pericytes relative to ECs (which previously completely inhibited capillary tube regression; Fig. 4). As shown in Fig. 5 B, at two different time points (3 or 6 d), siRNA suppression of EC TIMP-2 and pericyte TIMP-3 resulted in tube regression responses of the EC–pericyte cocultures. At later times of culture at 6 d, the suppression of EC TIMP-2 alone resulted in a tube regression response in a coculture containing 30% pericytes. At 3 d, the combination of EC TIMP-2 and pericyte TIMP-3 strongly induced capillary tube regression. In 50% pericyte cocultures, the only combination of siRNAs that affected tube regression was EC TIMP-2 combined with pericyte TIMP-3. This data strongly argues that both EC-derived TIMP-2 and pericyte-derived TIMP-3 are required for EC–pericyte cocultures to stabilize capillary tubes.

Identification of molecular targets of TIMP-2 and -3 that control capillary tube stabilization: MT1-MMP is a key regulator of EC tube formation and invasion responses

A key question in our studies is what molecular targets are blocked by TIMP-2 and -3 that interfere with both tube formation (Fig. 1) as well as the tube regression response (Fig. 4). To address this issue, we performed experiments with a series of potential targets of these TIMPs using an siRNA suppression approach. As shown in Fig. 6, we have suppressed the protein expression of a variety of MT-MMPs as well as ADAM proteinases and
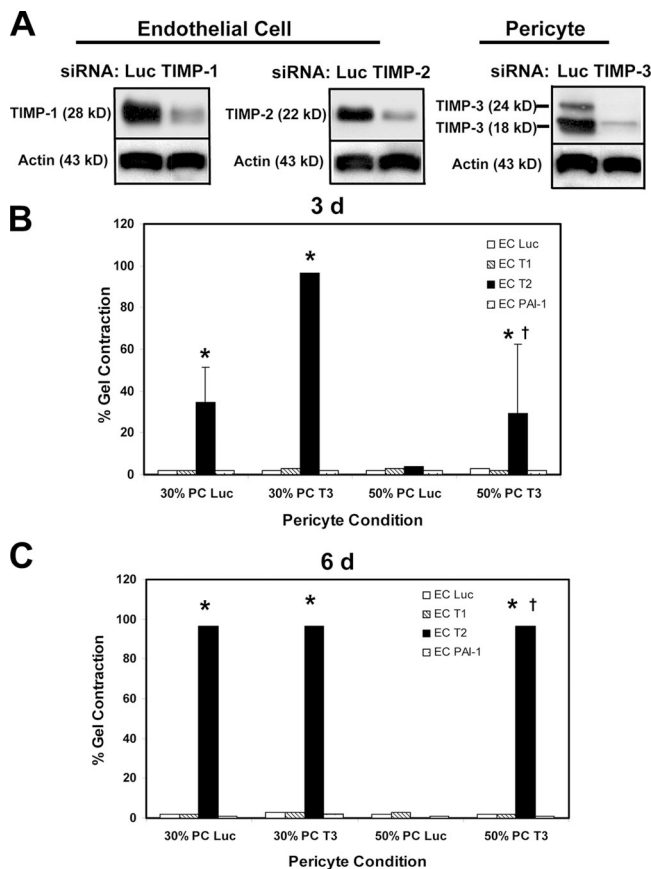
A

Endothelial Cell   Pericyte

siRNA: Luc TIMP-1   siRNA: Luc TIMP-2   siRNA: Luc TIMP-3

TIMP-1 (28 kD)

Actin (43 kD)

TIMP-2 (22 kD)

Actin (43 kD)

TIMP-3 (24 kD)
TIMP-3 (18 kD)

Actin (43 kD)

B 3 d

C 6 d

Figure 5. **EC-derived TIMP-2 and BRP-derived TIMP-3 are required for EC–pericyte interactions to stabilize EC tube networks.** ECs were transfected with siRNAs targeting TIMP-1, TIMP-2, PAI-1, or luciferase control (Luc), and BRPs were transfected in a similar manner with siRNAs targeting TIMP-3 or luciferase control. (A) Western blot analysis of EC-conditioned media and BRP cell lysates indicates the effectiveness of siRNA treatment on the expression of the indicated TIMPs as well as actin controls. (B and C) ECs were suspended in collagen matrices in the presence of 30 or 50% BRPs (relative to ECs) in the indicated combinations. EC tube network regression was induced with 1 µg/ml of activated human plasmin and was quantitated at 3 or 6 d (reported as the mean percentage of gel contraction ± SD [error bars]). *, P < 0.01 compared with luciferase control; †, P < 0.01 for EC TIMP-2 siRNA–treated ECs compared with other samples with 50% BRPs. PC, pericyte.

performed tube formation experiments using the vasculogenic assay system. Western blots show strong protein suppression of key enzymes (along with actin control) with biological activity in our system (Figs. 6 and 7). There was complete specificity in this suppression in that only the indicated siRNA suppressed the expression of the appropriate protein and had no influence on any of the other proteinases using Western blot analysis. The MT1-MMP siRNA is shown to markedly block tube and lumen formation compared with luciferase control and MT3-MMP siRNAs (Fig. 6 A). Interestingly, the morphology of MT1-MMP siRNA–treated cells looks remarkably similar to ECs treated with TIMP-2 or -3 as shown in Fig. 1 and in Videos 1–5. MT1-MMP siRNA–treated ECs extend fine processes into the 3D collagen matrices but fail to form lumenal structures or tube networks. Quantitation of these results reveals that only MT1-MMP siRNA had a strong blocking influence (Fig. 7 A). In contrast, no other siRNA had a blocking influence, and ADAM-9 siRNA actually stimulated the

EC lumen formation process, suggesting that it may normally be an inhibitor of these events. Overall, these data strongly show that the likely key target of TIMP-2 and -3 in vasculogenesis assays is MT1-MMP, which is known to be blocked by these two TIMPs (Baker et al., 2002). The inability of TIMP-1 to block in these assays also supports this conclusion because it has no ability to block MT1-MMP (Baker et al., 2002).

To further confirm this conclusion, we performed ELISA capture assays using GFP epitope-tagged MT1-MMP or TIMP-3 to demonstrate binding interactions between the two proteins. As shown in Fig. 6 C, the strong binding of TIMP-2 and -3 is detected to GFP epitope-tagged MT1-MMP by capturing the complex on anti-GFP–coated wells in HEK293 cell cotransfection experiments. The reverse experiment also shows the binding of MT1-MMP to TIMP-3 in ECs when a TIMP-3–GFP fusion protein is expressed in ECs using a recombinant adenovirus. TIMP-3–GFP is captured onto wells, and the wells were probed with anti–MT1-MMP antibodies to reveal the binding interaction (Fig. 6 C).

To further analyze the influence of these metalloproteinase siRNAs, we performed two additional assays that mimic the process of angiogenesis whereby ECs invade into collagen matrices from a matrix surface (Davis et al., 2002; Davis and Senger, 2005). For these assays, we used two distinct stimuli to induce EC invasion and tube morphogenesis in 3D collagen matrices. We previously reported that sphingosine-1 phosphate (S1P) induces EC invasion (Bayless and Davis, 2003), and, here, we report for the first time that the chemokine stromal-derived factor-1α (SDF-1α) strongly induces invasion and tube morphogenesis in our system when it is incorporated into a 3D collagen matrix. This latter chemokine is known to synergize with VEGF in both developmental and pathological vascular morphogenic events (Ceradini et al., 2004; Kryczek et al., 2005). It may represent a more physiologically relevant stimulus than S1P in this type of assay system.

As shown in Fig. 7, MT1-MMP siRNA dramatically blocks the invasion stimulated by either S1P or SDF-1α. This is shown quantitatively in Fig. 7 (B and C) and through photographs in Figs. S4 and S5 (available at http://www.jcb.org/cgi/content/full/jcb.200603176/DC1). Interestingly, MT2-MMP siRNA also inhibits SDF-1α invasion while partially inhibiting S1P invasion. Interestingly, ADAM-15 siRNA suppresses invasion selectively with SDF-1α–induced responses. ADAM-9 siRNA stimulates invasion responses like the aforementioned vasculogenesis assay, whereas ADAM-17 siRNA partially stimulates the SDF-1α invasion response. Collectively, these data show that MT1-MMP is required for EC tube formation in vasculogenic assays as well as in invasion and tube morphogenesis in response to two strong invasion-promoting stimuli, SDF-1α and S1P. Both MT2-MMP and ADAM-15 appear to play a lesser but detectable role selectively in SDF-1α–induced EC invasion responses.

MMP-1, MMP-10, and ADAM-15 regulate capillary tube regression responses in 3D collagen matrices

To address the role of various metalloproteinases in the capillary tube regression response, we performed regression time courses with the siRNA-treated ECs over time (Fig. 8 A).
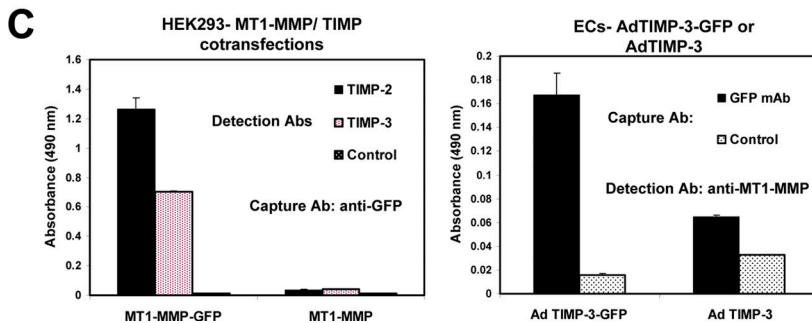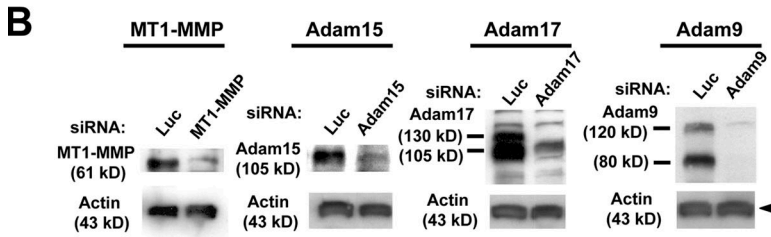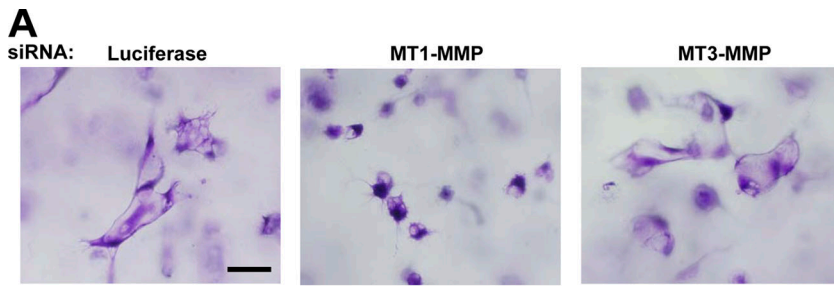
Figure 6. MT1-MMP is a TIMP-2 and -3 target required for EC tubular network formation in 3D collagen matrices. ECs were treated with the indicated siRNAs and suspended in 3D collagen matrices for 48 h before fixation for photography or quantitation. (A) Representative fields of ECs treated with MT1-MMP, MT3-MMP, or luciferase control siRNAs. Bar, 100 μm. (B) ECs transfected with the indicated siRNAs were cultured for 24 h before the preparation of lysates for Western blot analysis of the indicated proteinases or actin control (arrowhead). (C) ELISA capture assay showing interactions of MT1-MMP with TIMP-2 and -3. (left) HEK293 cells were cotransfected with MT1-MMP–GFP fusion or MT1-MMP alone with TIMP-2, -3, or control plasmids, and lysates were made after 20 h. Lysates were incubated in microwells coated with an anti-GFP mAb and were probed with antibodies to TIMPs to detect binding interactions. (right) ECs were infected overnight with recombinant adenoviruses carrying TIMP-3–GFP or TIMP-3 alone, and lysates were prepared. Lysates were incubated in microwells coated with an anti-GFP mAb and were probed with an MT1-MMP antibody to detect binding interactions. Error bars represent SD.

Marked delays in the regression response occurred with three siRNA treatments: MMP-1, MMP-10, and ADAM-15 (Fig. 8 A). Previously, we reported that MMP-1 and -10 both control capillary tube regression (Saunders et al., 2005). ADAM-15, a known TIMP-3 target, appears to play a strong role in this process as well. A partial delay occurred with MT1-MMP–treated cells, which may relate to the fact that these cells fail to undergo substantial tube formation. EC tube formation is not blocked with MMP-1–, MMP-10–, or ADAM-15–treated cells. Interestingly, ADAM-9– and -17–treated ECs show accelerated regression responses compared with control luciferase as well as ADAM-10 and -12 treatments.

To address how these treatments affect pro–MMP-1 or -10 activation, Western blots were performed (Fig. 8 B). MMP-1 and -10 siRNA knockdown shows marked suppression of the respective proteins, whereas ADAM-15 knockdown appears to suppress the overall levels of both pro–MMP-1 and -10 as well as the activated forms of these two enzymes, which appears to account for the regression delay. The mechanism by which ADAM-15 suppression affects MMP-1 or -10 levels and activation is unclear. Interestingly, ADAM-9 and -17 suppression appears to accelerate the regression response by affecting MMP-1 activation, whereby a greater proportion of activated pro–MMP-1 is observed in both cases. Overall, these data suggest that three primary enzymes appear to play a central, required role in the MMP-dependent regression response (MMP-1, MMP-10, and ADAM-15). These metalloproteinases are all blocked by

TIMP-3, whereas MMP-1 and -10 are known to be blocked by TIMP-2.

The ability of TIMP-3 to stabilize tubes is dependent on its proteinase inhibitory activity

To further confirm that TIMP-3 acts as a stabilizing factor through blocking metalloproteinase targets, we performed site-directed mutagenesis of TIMP-3 using known mutations that interfere with its proteinase inhibitory activity (Langton et al., 1998; Brew et al., 2000). We mutated either cysteines 1, 3, or both and made lentiviral vectors that express these constructs in comparison with TIMP-1. Stable EC cell lines expressing these recombinant proteins were selected, and each of the respective recombinant proteins were produced at appropriate levels (Fig. 9 A). To address whether the recombinant proteins influence tube formation or regression, we performed various biologic assays (Fig. 9, B–D). As shown in Fig. 9, TIMP-3 wild type is able to block lumen formation (Fig. 9 B), invasion responses (Fig. 9 C), and capillary tube regression (Fig. 9 D). In contrast, increased TIMP-1 expression fails to block tube formation or invasion but completely inhibits tube regression through its known ability to inhibit MMP-1– and -10–dependent proteolytic events (Davis et al., 2001; Baker et al., 2002). The TIMP-3 mutants failed to block EC lumen formation or invasion, suggesting that the proteinase inhibitory function of TIMP-3 is required for the ability of TIMP-3 to stabilize tubes through interference with EC tube morphogenesis.
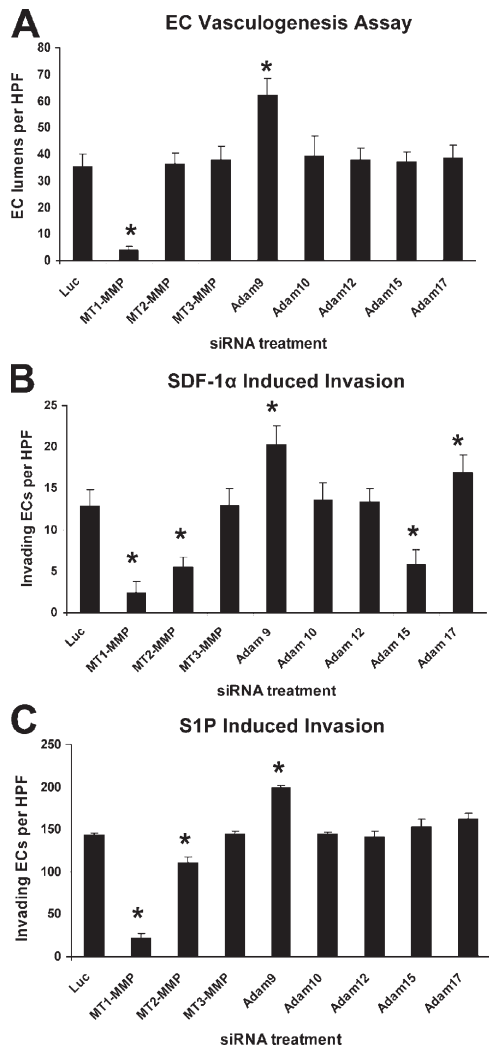
A EC Vasculogenesis Assay

B SDF-1α Induced Invasion

C S1P Induced Invasion

Figure 7. **MT1-MMP is required for EC tube network formation as well as invasion and tube formation stimulated by SDF-1α and S1P.** (A–C) ECs were treated with the indicated siRNAs and were cultured within collagen matrices (A) or on the surface of collagen matrices containing either SDF-1α (B) or S1P (C) to stimulate invasion. Quantitation of each condition occurred at either 24 (C) or 48 h (A and B). (A) Data are reported as the mean number of EC lumens per high-powered field (HPF; A) or invading ECs per high-powered field (B and C) $\pm$ SD (error bars; $n = 3$). *, $P < 0.01$ compared with luciferase control.

Surprisingly, the TIMP-3 C1S mutant retained its ability to block tube regression responses, whereas the TIMP-3 C3S mutant or C1SC3S double mutant did not. Overall, these data demonstrate that the proteinase inhibitory function of TIMP-3 is central to its ability to stabilize tubes through the blockade of tube morphogenesis and tube regression responses.

Discussion

EC-derived TIMP-2 and pericyte-derived TIMP-3 coregulate human capillary tube stabilization in 3D collagen matrices

There is considerable interest in the mechanism by which pericytes stabilize capillary tubes during development and other vascular morphogenic events (Orlidge and D'Amore, 1987;

A Plasminogen Induced Regression

B

MMP-1

MMP-10

siRNA: Luc MT1-MMP MMP-1 MMP-10 Adam 9 Adam 10 Adam 12 Adam 15 Adam 17

MMP-1 (51 kD)

MMP-10 (54 kD)

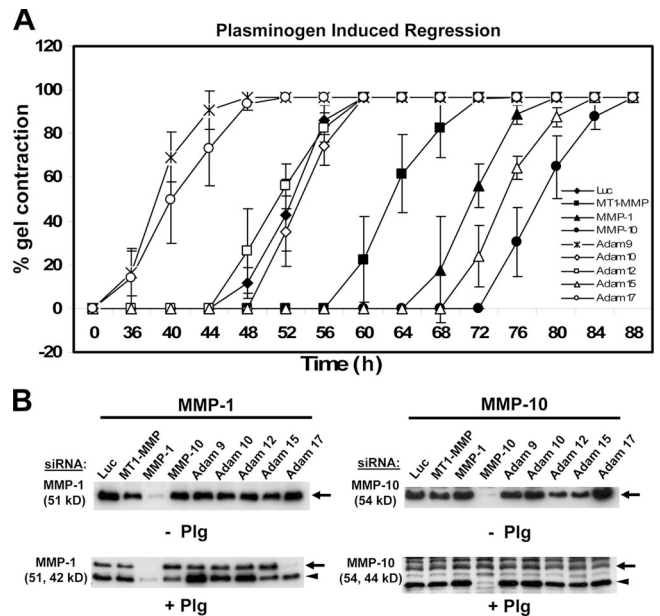− Plg

MMP-1 (51, 42 kD)

MMP-10 (54, 44 kD)

+ Plg

Figure 8. **MMP-1, MMP-10, and ADAM-15 represent TIMP-2 and -3 targets involved in EC tubular network regression.** ECs were transfected with the indicated siRNAs, suspended in 3D collagen matrices, and cultured in the presence of 2 µg/ml Plg to initiate EC tubular network regression. (A) Cultures were monitored every 4 h for tube regression and collagen gel contraction. Data are reported as the mean percent gel contraction $\pm$ SD (error bars; $n = 8$). (B) At 96 h, conditioned media from control cultures (no Plg) or Plg-treated cultures (+Plg) were collected and analyzed by Western blot analysis for MMP-1 and -10 proenzyme (arrow) and activation (arrowhead) levels.

Jain, 2003; von Tell et al., 2006). Much data support the concept that pericytes stabilize EC-lined tubes as a result of observations that tubes without associated pericytes are more susceptible to regression (Jain, 2003; von Tell et al., 2006). However, the molecular mechanisms that regulate these phenomena remain unclear. The data presented here propose a new concept in that pericyte-induced capillary tube stabilization can be mediated, in part, by proteinase inhibition (Fig. 10). Our work suggests that proteinase inhibition of both EC tube morphogenesis (leading to the cessation of morphogenesis) and tube regression is necessary to control tube stabilization.

Previous data from our laboratory support the concept that ECs undergoing the lumen formation process and assembling into 3D networks induce a gene program to regulate tube formation but also establish the conditions necessary for tube regression (Bell et al., 2001; Davis et al., 2002; Davis and Saunders, 2006). In studies of EC network collapse of 3D collagen matrices, ECs secrete high levels of a latent collagenase, pro–MMP-1, as well as pro–MMP-10 during the assembly of 3D tubular networks (Davis et al., 2001; Saunders et al., 2005), which we have shown are proregression agents. In the presence of serine proteinases, MMP-1 and -10 zymogen activation occurs, and active MMP-1 controls collagen and ECM dissolution and collapse of capillary networks. This regression event is completely blocked by the presence of sufficient pericytes (i.e., to deliver TIMP-3; Figs. 3–5) or the addition of exogenous TIMP-3 or -2 (Fig. 1 and Fig. S2). These observations all support the concept that the regulation of proteinase activity during angiogenesis
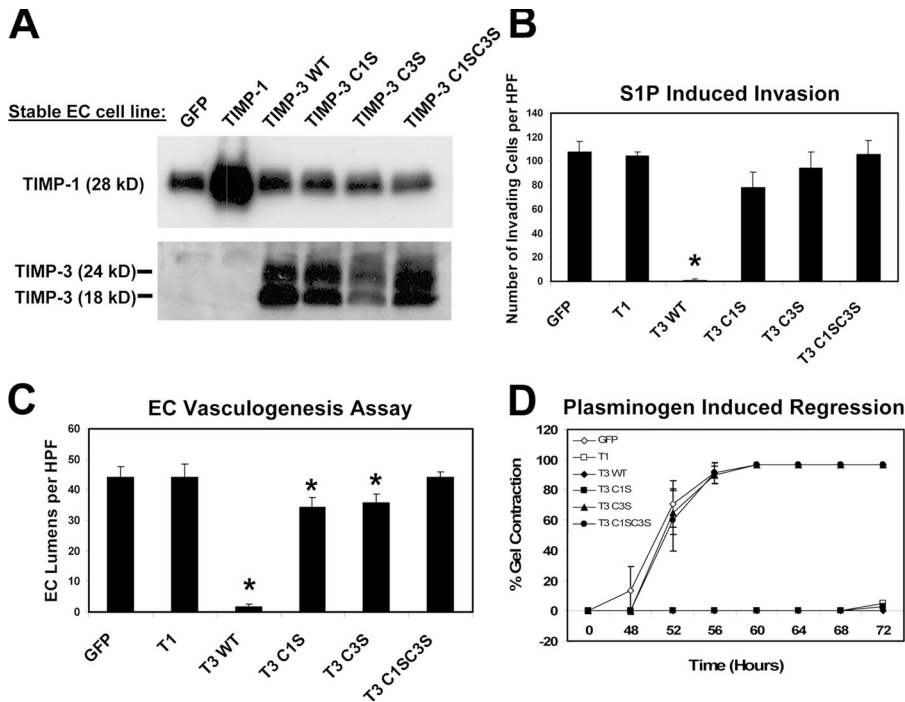
Figure 9. **The proteinase inhibitory activity of TIMP-3 is required for tube stabilization through its ability to inhibit EC invasion, tube formation, and regression.** Generation of stable EC cell lines expressing GFP, TIMP-1 (T1), TIMP-3 (T3) wild-type (WT), and mutants is described in Materials and methods. (A) EC-conditioned media or cell lysates were analyzed for TIMP-1 and -3 levels via Western blot analysis. (B) Stable EC cell lines with the indicated expressed constructs were placed on 3D collagen matrices and stimulated to invade with S1P for 48 h, and, after fixation, the invasion response was quantitated ($n = 3$). (C) The indicated stable EC cell lines were suspended within 3D collagen matrices and allowed to undergo EC tubular network formation for 48 h. After fixation, lumen formation was quantitated. (B and C) *, $P < 0.01$ compared with GFP control. (D) EC cell lines were suspended as in C and were cultured in the presence of 2 µg/ml Plg. Cultures were monitored every 4 h for EC tube regression and collagen gel contraction. Data are reported as the mean percent gel contraction ± SD (error bars; $n = 8$). HPF, high-powered field.

(e.g., during wound healing) must be tightly controlled to prevent the regression of newly formed vascular networks. A similar conclusion was reached in studies of a mouse knockout of the MMP inhibitor RECK. An embryonic lethal phenotype occurs at E10.5 secondary to excessive collagenase activity, vascular collapse, and hemorrhage (Oh et al., 2001). Marked destruction of the collagen scaffold was observed in vivo and was associated with defects in vascular tube networks in a manner that was remarkably similar to our previous studies (Davis et al., 2001; Saunders et al., 2005).

Our work here shows that distinct metalloproteinases, including members of the MMP and ADAM families, influence promorphogenic versus proregression events (Fig. 10). Furthermore, this study shows that EC-derived TIMP-2 and pericyte-derived TIMP-3 play direct roles in regulating these stabilizing effects by inhibiting specific MMPs and ADAMs. EC-derived molecular targets for TIMP-2 and -3 include MT1-MMP, which appears to be the major regulator of EC tube morphogenesis by controlling EC invasion and lumen formation. In addition to MT1-MMP, we show that MT2-MMP and ADAM-15 appear to contribute to tube morphogenesis by regulating the EC invasion of collagen matrices. Other targets include MMP-1, MMP-10, and ADAM-15, which act together to regulate capillary tube regression.

Pericyte-derived TIMP-3 inhibits EC tube formation and vascular assembly in vitro and in vivo and stabilizes preexisting EC tubular networks

TIMP-3 has previously been reported as an antiangiogenic agent and also inhibits the growth of solid tumors (Anand-Apte et al., 1997; Spurbeck et al., 2002; Qi et al., 2003). Interestingly, TIMP-3 is frequently down-regulated by various tumors through methylation of its promoter (Wild et al., 2003). In this study,

we show that TIMP-3 prevents EC tubular morphogenesis in 3D matrices in vitro as well as vasculogenesis and vascular remodeling in vivo (Figs. 1 and 2). Importantly, TIMP-3 expression from pericytes was strongly induced by the presence of ECs (Fig. 3, A and B) in 3D collagen matrices. We show that siRNA suppression of TIMP-3 in pericytes markedly diminishes their ability to stabilize EC-lined tubes that are susceptible to
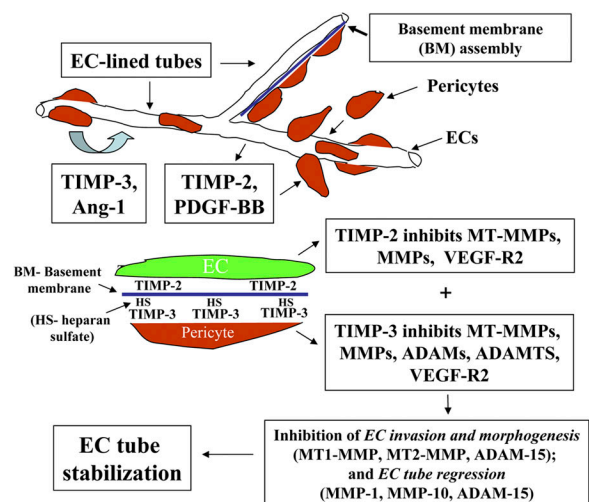

Figure 10. **Schematic diagram illustrating the contribution of TIMP-2 and -3 to pericyte-induced vascular tube stabilization.** As shown, TIMP-2 is derived from ECs, whereas TIMP-3 is produced by pericytes. Together, they contribute to vascular stabilization by inhibiting a variety of MMPs, ADAMs, and VEGFR-2. The initiation of tube stabilization requires the blockade of both EC tube formation and EC tube regression, which further leads to the cessation of EC activation and the development of EC quiescence. We hypothesize that pericytes are required for ECs to assemble basement membrane matrices, which locally capture and present TIMP-3 to ECs through heparan sulfate proteoglycans such as perlecan.

MMP-1–, MMP-10–, and ADAM-15–dependent tube regression (Figs. 3–5). This suppression was selective for pericytes because ECs in our system do not express TIMP-3, and this siRNA also had no effect when ECs were treated with it. Site-directed mutagenesis of TIMP-3 using treatments known to eliminate the proteinase activity of various TIMPs (Brew et al., 2000) interfered with its ability to block both tube formation and regression, showing that these activities depend on its proteinase inhibitory function. Pericytes produce TIMP-3 to inhibit EC MT1-MMP, MT2-MMP, and ADAM-15, which we have identified as important targets controlling tube morphogenesis. Previous studies have revealed important roles for MT1-MMP and ADAM-15 in vascular morphogenic events (Horiuchi et al., 2003; Chun et al., 2004). A final point concerns the known ability of TIMP-3 to strongly interact with ECM, such as heparan sulfate in vascular basement membrane matrices (Fig. 10; Davis and Senger, 2005). This unique ability of TIMP-3 among the TIMPs (Baker et al., 2002) is likely to be important in vascular stabilization because of the fact that it will be presented as a component of the basement membrane matrix in direct contact with endothelium and pericytes in stabilized vessels.

EC-derived TIMP-2 is a regulator of EC tube stabilization in 3D collagen matrices

Previous studies indicate that TIMP-2 can block angiogenesis through a nonproteinase inhibitory mechanism by binding the $\alpha3\beta1$ integrin and activating signaling events leading to the inhibition of VEGF receptor-2 (VEGFR-2) signaling (Seo et al., 2003; Stetler-Stevenson and Seo, 2005). In this study, TIMP-2 appears to block in a similar manner to TIMP-3 (Fig. 1) or to chemical inhibitors of surface metalloproteinases such as GM6001 (Videos 1–5). In our model, the inhibitory functions and vascular stabilizing functions of TIMP-2 appear to occur through its proteinase inhibitory function. Supporting this conclusion, the siRNA suppression of MT1-MMP expression, a key TIMP-2 and -3 target, markedly blocks EC tube formation (Fig. 6), and the morphology of MT1-MMP siRNA–treated ECs appears remarkably similar to ECs treated with either TIMP-2 or -3 in 3D collagen matrices (Figs. 1 C and 6). Furthermore, siRNA suppression of TIMP-2 expression in ECs can lead to destabilization and MMP-1–dependent regression of EC–pericyte cocultures (Fig. 5). Overall, our work with TIMP-2 as well as TIMP-3 supports the concept that both TIMPs play a role in the stabilization of newly formed vessels in 3D matrices.

In addition, TIMP-3 (like TIMP-2) has been reported to inhibit VEGFR-2 signaling (Qi et al., 2003). The inhibition of VEGFR-2 is a major therapeutic target in antiangiogenic protocols to inhibit excess vascularization in tumors and other contexts (Jain, 2005). Interestingly, recent data suggest that treatment of angiogenic fields with VEGFR-2 antagonists results in the regression of select vessels followed by the normalization of vasculature, which is a step toward stabilization (Jain, 2003, 2005). Thus, both TIMP-2 and -3 have been reported to regulate VEGFR-2 in addition to their proteinase inhibitory activity. Our work extends these observations in that TIMP-2 and -3 can act as vascular stabilizing agents by blocking distinct proteinases required for tube morphogenesis and regression

(Fig. 10). Thus, this study, coupled with previous studies (Qi et al., 2003; Seo et al., 2003), suggests that EC-derived TIMP-2 and pericyte-derived TIMP-3 act through several distinct mechanisms to facilitate vascular stabilization.

Finally, we observe that ECs will continuously undergo morphogenesis and lumen formation in 3D matrices unless they are provided with a stabilization or stop signal. Without this signal, proteinase activities eventually result in the regression of EC networks. This concept is consistent with a proposed target hypothesis (Davis et al., 2002) whereby ECs (in a similar fashion to neurons) search for or recruit a target cell that provides a stabilizing signal. Pericytes appear to provide this target function for EC tube networks, which shifts the molecular balance from morphogenesis or regression toward tube stabilization.

Materials and methods

Reagents
Purified human Plg was obtained from American Diagnostica, Inc. VEGF and bFGF were purchased from Upstate Biotechnology. Activated human plasmin was obtained from Calbiochem. Purified TIMP-1 (CC3328) and -2 (CC3327) were obtained from Chemicon. Recombinant human TIMP-3 (973-TM) and human SDF-1α (CXCL12) were obtained from R&D Systems, and the metalloproteinase inhibitor GM600 was obtained from Calbiochem. D-erythro-S1P was obtained from Avanti Polar Lipids, Inc. A blocking antibody targeting $\alpha2$ integrin (BHA2.1) was purchased from Chemicon, and a blocking antibody against $\alpha5$ integrin (mAb 16) was purchased from Becton Dickinson. Antibodies targeting MMP-10 (mAb 9101), TIMP-1 (AF970), TIMP-2 (AF971), ADAM-9 (AF949), and ADAM-15 (AF945) were obtained from R&D Systems. Antibodies targeting ADAM-12 (AB 19133), ADAM-17 (AB 19027), and TIMP-3 (mAb 3318) were obtained from Chemicon. A polyclonal antibody against human MT1-MMP (RP1–MMP-14) was purchased from Triple Point Biologics. The PAI-1 polyclonal antibody, MMP-1 mAb (IM35L), and actin mAb (CP01) were purchased from Calbiochem. Oligonucleotide primers were obtained from Sigma-Genosys. All other reagents were purchased from Sigma-Aldrich unless otherwise noted. The pAdEasy adenoviral system was obtained from B. Vogelstein (Johns Hopkins Medical School, Baltimore, MD), and the mRFP construct was obtained from R. Tsien (University of California, San Diego, La Jolla, CA).

Cell culture
Human umbilical vein ECs (HUVECs) were purchased from Cambrex and were used from passage 2–6. BRPs were cultured in DME containing 10% FBS in gelatin-coated flasks.

BRP isolation
Bovine eyes were obtained from the Rosenthal Center (Texas A&M University), transported on ice, and submerged in Betadine for 10 min before retinas were dissected and placed into sterile buffer. The isolation protocol was essentially as previously described (Nayak et al., 1988). At confluence, pericytes were screened for the expression of 3G5 antigen and α-smooth muscle actin.

EC invasion, lumen formation, and regression assays
ECs were placed in 3D invasion assays as described previously (Bayless and Davis, 2003), in which ECs invade into 3.75 mg/ml of collagen matrices containing either 1 μM S1P or 200 ng/ml SDF-1α. Alternatively, lumen formation assays were used where individual ECs were suspended within 3.75 mg/ml of collagen type I matrices and allowed to assemble into 3D networks over time (Davis et al., 2002). Cultures were fixed at indicated time points with 3% glutaraldehyde in PBS, pH 7.5, for at least 30 min before additional manipulation. In some cases, cultures were stained with 0.1% toluidine blue in 30% methanol and were destained before visualization and photography. Conditioned media were collected to examine differential protein expression at various time points. Conditioned media were run on SDS-PAGE gels, transferred to polyvinylidene membranes, probed, and developed. 3D collagen gels were also extracted in some cases to examine protein expression.

Regression assays were performed as described previously (Saunders et al., 2005). For quantitative analysis of gel contraction, 15-μl mixtures of ECs and collagen matrix (n = 8 cultures per condition) were placed in 384-well tissue culture plates (VWR Scientific Products). Cultures were allowed to equilibrate for 30 min before the addition of media with or without the serine proteases Plg or plasmin. The addition of culture media denoted time zero, and cultures were monitored every 4 h for gel contraction. Upon initiation of gel contraction, gel area was recorded using an ocular grid, and percent collagen gel contraction was calculated as follows: [(original area − current gel area)/original area] × 100. When contraction was complete, cultures were fixed or extracted, and media was examined for MMP expression and activity. Data are reported as the mean percent gel contraction ± SD.

Coculture experiments

Confluent ECs were resuspended in 3.75 mg/ml of 3D collagen matrices at a final concentration of 10^6 cells/ml. BRPs were incorporated into collagen matrices at varying ratios as indicated. EC or EC/PC cocultures (15-μl vol) were evaluated in EC tubular network formation or quantitative regression assays performed in 384-well plates as previously described (Saunders et al., 2005).

Transfection of ECs and pericytes with siRNA

Custom smart pool siRNAs for TIMP-3 and luciferase controls were purchased from Dharmacon and were resuspended (40 μM) in universal buffer and stored at −80°C. siGenome siRNAs targeting TIMP-1, -2, -4, and PAI-1 were obtained from Dharmacon and prepared. Transfection of ECs with siRNAs before use in experiments was performed essentially as described previously (Saunders et al., 2005). Transfection of BRPs with siRNAs was performed in a similar manner except that LipofectAMINE 2000 (Invitrogen) was used for transfection. Cells were transfected at a final siRNA concentration of 200 nM.

Mouse embryo culture

CD1 wild-type mouse embryos were dissected at E7.5 and cultured for 48 h in a continuous gas (5% CO_2) rolling embryo culture apparatus. Media (0.5 ml/embryo) was changed after 24 h and contained high glucose (4.5 g/L) DME (Invitrogen) with 75% immediately centrifuged rat serum (Harlan) and glutamine-penicillin-streptomycin (Invitrogen). Recombinant TIMP-1 (Chemicon) and -3 (R&D Systems) were added to culture media at 5 μg/ml, and GM6001 (Calbiochem) was added at 5 μM. Embryos were photographed live before whole mount staining with VE-cadherin antibodies (BD Biosciences). RT-PCR analysis and immunohistochemistry were performed as previously described (Lai et al., 2003; Bohnsack et al., 2004). Primers used for this analysis are as follows: HPRT, upstream primer (UP) (GCTGGTGAAAAGGACCTCT) and downstream primer (DN) (CACAGG-ACTAGAACACCTGC); TIMP-1, UP (CGAATCAACGAGACCACCTT) and DN (TGCAGGCATTGATGTGAAAT); and TIMP-3, UP (CACGGAAGCCTC-TGAAAGTC) and DN (CCCAAAATTGGAGAGCATGT).

Preparation of vectors and stable cell lines: cloning and preparation of lentiviral vectors

TIMP-1 was amplified from HUVEC cDNA (Bell et al., 2001) using the primers TIMP-1 HindIII UP (5′-AGAAGCTTCGAGATCCAGCGCCCAGAG-3′) and TIMP-1 EcoRV DN (5′-AGGATATCGCAGGCTTCAGTTCCACTC-3′). TIMP-3 was amplified from human placental cDNA (BD Biosciences and CLONTECH Laboratories, Inc.) using the primers TIMP-3 XhoI UP (5′-AGCTC-GAGGCAATGACCCCTTGGCTCGGGCTCATC-3′) and TIMP-3 XbaI DN (5′-AGTCTAGACGCTCAGGGGTCTGTGGCATTG-3′). Both inserts were initially cloned into the pAdTrack-CMV vector using similar methods that we have described previously (Bell et al., 2001). Positive clones were sequenced, and protein expression was verified via Western blotting.

The production of recombinant lentivirus was accomplished using the pLenti6/V5 TOPO cloning system (Invitrogen). TIMP-1 was amplified from the pAdTrack-CMV vector using the primers TIMP-1 pLenti UP (5′-CACCATG-GCCCCCTTTGAGCCCCTG-3′) and TIMP-1 pLenti DN (5′-AGGATATCGCA-GGCTTCAGTTCCACTC-3′). TIMP-3 was amplified from the pAdTrack-CMV vector using the primers TIMP-3 pLenti UP (5′-CACCATGACCCCCTTGGCTC-GGGCTC-3′) and TIMP-3 pLenti DN (5′-AGTCTAGACGCTCAGGGGTCT-GTGGCATTG-3′). Enhanced GFP was amplified from the pEGFP-N2 vector (CLONTECH Laboratories, Inc.) using the primers GFP pLenti UP (5′-CAC-CATGGTGAGCAAGGGCGAGG-3′) and GFP pLenti DN (5′-AGTCTAGA-TTACTTGTACAGCT-CGTCCATGC-3′). The sequence encoding a modified mRFP was amplified from the vector pRSETB (Campbell et al., 2002) using the primers mRFP pLenti UP (5′-CACCATGGCCTCCTCCGAGGACGTC-3′)

and mRFP pLenti DN (5′-AGTTAGGCGCCGGTGGAGTGGCG-3′). Once amplified, each insert was TOPO cloned into the pLenti6/V5 TOPO vector. After TOPO cloning, One Shot Stbl3 Chemically Competent *Escherichia coli* (Invitrogen) were transformed with DNA according to the manufacturer's protocol. Individual clones containing TIMP-1, TIMP-3, GFP, and mRFP inserts were verified via PCR and sequence analysis.

A QuikChange XL Site-Directed Mutagenesis Kit was obtained from Stratagene and used to mutate the proteinase inhibitory domain of TIMP-3. PAGE-purified primers (Sigma-Genosys) were generated as follows: TIMP-3 C1S UP (5′-GCGCCGAGGCGTCCACATGCTCGCCCAGCCAC-3′) and TIMP-3 C1S DN (5′-GTGGCTGGGCGAGCATGTGGACGCCTCGGCGC-3′); TIMP-3 C3S UP (5′-GCGCCGAGGCGTGCACATCCTCGCCCAGCCAC-3′) and TIMP-3 C3S DN (5′-GTGGCTGGGCGAGGATGTGCACGCCTCGGCGC-3′); and TIMP-3 C1SC3S UP (5′-GCGCCGAGGCGTCCACATCCTCGCCCAGC-CAC-3′) and TIMP-3 C1SC3S DN (5′-GTGGCTGGGCGAGGATGTGGAC-GCCTCGGCGC-3′). Site-directed mutagenesis was performed according to the manufacturer's protocol. Mutated clones were verified via restriction digestion, plasmid sequencing, and Western blot analysis.

The 293FT lentiviral packaging cell line was obtained from the ViraPower Lentiviral Gateway Expression Kit (Invitrogen). 293FT cell lines were cultured as recommended by the manufacturer in 500 μg/ml G418. TIMP-1, -3, wild-type, and mutant isoforms as well as GFP and mRFP lentiviruses were produced according to the manufacturer's protocol. In brief, a T75 flask containing 80% confluent 293FTs in 5 ml of antibiotic-free DME/10% FCS was transfected with 4 μg pLenti6/V5-D-TOPO vector and 12 μg Virapower (Invitrogen) using 36 μl LipofectAMINE 2000 (Invitrogen) in 3 ml OptiMEM transfection medium (Invitrogen). The following morning, media was removed, and 12 ml of antibiotic-free DME/10% FCS was supplied. 293FT cells were allowed to produce lentivirus for 48 h. Media containing live lentivirus was collected and spun to remove cell debris before storage at −70°C. Low passage HUVECs or BRPs were allowed to grow to 80% confluency in T75 flasks. Cells were infected with lentivirus at the following ratio: 3 ml of cell culture media, 6 ml lentiviral supernatant, and polybrene (hexadimethrine bromide) at a final concentration of 12 μg/ml. Cells were infected for 6 h in this media mixture before the addition of another 6 ml of cell culture media. Cells were incubated for 72 h before the aspiration of media and initiation of stable cell line selection using Blasticidin (Invitrogen) at a final concentration of 5 (HUVECs) or 15 μg/ml (BRPs). Cells were cultured in the presence of Blasticidin for 10–14 d to ensure stable cell line selection. The expression of respective proteins was verified via Western blot analysis.

Generation of TIMP-3 and MT1-MMP GFP fusion constructs and TIMP-3/TIMP-3–GFP adenoviruses

MT1-MMP was amplified from plasmid EX-M0327-M02 (Genecopoeia) containing the full-length cDNA for human MT1-MMP (MMP-14). Standard restriction digestion cloning was performed to clone MT1-MMP into pAdTrack-CMV using the primers MT1-MMP HindIII UP (5′-AGAAGCTTGCCACCATGTCTC-CCGCCCCAAGACCC-3′) and MT1-MMP EcoRV DN (5′-AGGATATCTCA-GACCTTGTCCAGCAGGGAAC-3′). A positive MT1-MMP pAdTrack clone was used as a source template to clone MT1-MMP into the pEGFP-N2 fusion vector (CLONTECH Laboratories, Inc.) using the primers MT1-MMP N2 HindIII UP (5′-AGAAGCTTGCCACCATGTCTCCCGCCCCAAGACCCC-CC-3′) and MT1-MMP N2 EcoRI DN (5′-AGGAATTCGACCTTGTCCAGCA-GGGAACG-3′). Next, the MT1-MMP–GFP fusion construct was cloned into the pAdShuttle-CMV expression plasmid using the primers MT1-GFP Ad NotI UP (5′-AGGCGGCCGCGCCACCATGTCTCCCGCCCCAAGACCC-3′) and MT1-GFP Ad EcoRV DN (5′-AGGATATCTTACTTGTACAGCTCGTCCATG-3′). At each step, positive clones were verified via PCR, restriction digestion, and plasmid sequencing. Furthermore, protein expression was verified via plasmid transfection into HEK293 cells for Western blot analysis.

TIMP-3 pAdTrack-CMV was used as a template for the amplification of TIMP-3 via standard PCR for cloning into the pEGFP-N2 fusion vector (CLONTECH Laboratories, Inc.) using the primers TIMP-3 N2 XhoI UP (5′-AGCTCGAGGCAATGACCCCCTTGGCTCGGGCTCATC-3′) and TIMP-3 N2 BamHI DN (5′-AGGGATCCCGGGGTCTGTGGCATTGATGATG-3′). A positive TIMP-3–GFP clone was used as a template to amplify TIMP-3–GFP for standard cloning into the pAdShuttle-CMV adenoviral vector using the primers TIMP-3–GFP pAd Shuttle XhoI UP (5′-AGCTCGAGGCAATGA-CCCCTTGGCTCGGGCTCATC-3′) and TIMP-3–GFP pAd Shuttle EcoRV DN (5′-AGGATATCCGGGGTCTGTGGCATTGATGATG-3′). At each step, positive clones were verified using PCR, restriction digestion, and sequence analysis. Additionally, clones were transfected, and visualization of GFP fusion proteins was verified via fluorescent microscopy, transfection of plasmids into HEK293 cells, and Western blot analysis of TIMP-3 and TIMP-3–GFP proteins. Recombinant adenoviruses encoding TIMP-3 and TIMP-3–GFP

were generated from expression plasmids TIMP-3 pAdTrack-CMV and TIMP-3–GFP pAdShuttle-CMV via recombination with the pAdEasy adenoviral vector as described previously (Bell et al., 2001).

Cotransfection of TIMP-2, TIMP-3, and MT1-MMP constructs in HEK293 cells for ELISA

HEK293 cells were cultured to 95% confluence in DME/10% FCS in 12-well plates precoated with 20 µg/ml of collagen type I. LipofectAMINE 2000 was used to cotransfect cells with 750 ng pLenti plasmids encoding TIMP-2 or -3 in combination with 750 ng of plasmids MT1-MMP pAdTrack or MT1-MMP–GFP pAdShuttle encoding MT1-MMP or MT1-MMP–GFP (1.5 µg of total DNA per well). Transfected HEK293 cells were allowed to recover for 24 h, and transfection efficiency was verified via fluorescent microscopy. Detergent lysates of cotransfected HEK293 cells were made using chilled (4°C) 2% Triton X-100 in 1× TBS, pH 8.0, containing complete EDTA-free protease inhibitor cocktail tablets (Roche Diagnostics). Before cell lysis, 12-well plates were washed once with 1.0 ml of warm, serum-free DME and placed on ice. Each well was lysed with 500 µl of cold lysis buffer. Lysates were transferred to 1.7-ml Eppendorf tubes and incubated on ice for 20 min before centrifugation at 20,000 rpm for 20 min at 4°C to pellet-insoluble cellular debris. Supernatants were removed and stored at −70°C until use.

A mAb (3E6) against GFP used to capture GFP fusion proteins was obtained from Qbiogene. Polystyrene microwell plates (VWR Scientific Products) were precoated with or without 2 µg/ml anti-GFP antibody in PBS overnight at 4°C. The following morning, plates were warmed to room temperature, aspirated to remove residual GFP antibody, and blocked in Tris–Tween 20 detergent solution for 20 min. HEK293 cell cotransfection lysates were diluted 1:2 with Tris–Tween 20 containing 1% BSA and incubated at 100 µl/well vol for 2 h at room temperature. Lysates were aspirated, and plates were washed four times in Tris–Tween 20 before incubation with polyclonal antibodies (50 µl/well) against TIMP-2 or -3 (R&D Systems) diluted at 1:200 and 1:100, respectively, in Tris–Tween 20 and 1% BSA. In separate wells, a control antibody targeting MT1-MMP (Triple Point Biologics) was used to ensure the proper capture of MT1-MMP–GFP and not MT1-MMP pAdTrack. Additionally, conditioned media and lysates were assessed via Western blotting to ensure the proper protein expression of each transfection condition. Primary antibodies were incubated for 1 h at room temperature, aspirated, and plates were washed four times before the addition of HRP-conjugated secondary antibodies (50 µl/well; DakoCytomation) diluted 1:2,000 in Tris–Tween 20 and 1% BSA. Secondary antibodies were incubated for 30 min at room temperature before washing three times in Tris–Tween 20 and were washed twice in ddH₂O. ELISA plates were developed using a typical O-phenylenediamine substrate solution (100 µl/well) and stopped with 100 µl/well of 1 M sulfuric acid before the measurement of absorbance at 490 nm. Data are reported as the mean absorbance for duplicate wells and have been background corrected against control wells, which were not precoated with the capturing GFP mAb.

Infection of HUVECs with TIMP-3 and TIMP-3–GFP adenoviruses for ELISA capture and detection of EC-derived MT1-MMP

HUVECs were cultured to confluence in T25 flasks. Viral transformation of ECs with recombinant adenoviruses encoding TIMP-3 or TIMP-3–GFP fusion was performed as described previously (Bell et al., 2001). The following morning, transformation efficiency was assessed using fluorescent microscopy. Flasks were washed twice with 3 ml of warm M199, and detergent lysates of TIMP-3– and TIMP-3–GFP-producing ECs were prepared using 1.5 ml of cold lysis buffer per T25 flask. The ELISA capture technique was performed as described above except that for HUVEC lysates, TIMP-3–GFP was captured, and lysates were probed for the EC-derived target MT1-MMP. The MT1-MMP polyclonal antibody (Triple Point Biologics) was used at a 1:200 dilution. Data are reported as the mean absorbance for duplicate wells and have been background corrected against control wells, which were not precoated with the capturing GFP mAb.

Microscopy and imaging

A fluorescence inverted microscope (Eclipse TE2000-U; Nikon) was used to visualize EC invasion, vasculogenesis, and regression as well as immunofluorescence microscopy. Lenses used for time lapse included a CFI plan-Fluor 20× with an NA of 0.45, whereas for immunofluorescence, a CFI plan-Apo 60× oil objective with an NA of 1.4 was used. FITC and rhodamine were used for immunofluorescence, whereas GFP and mRFP were used for still photographs of EC–pericyte cocultures. Imaging media included Slow Fade (Invitrogen) for immunofluorescence and M199 culture

media without phenol red for all time lapses of EC cultures and still photography of EC–pericyte cultures. Imaging of cocultures used an inverted microscope (CKX41; Olympus) and 20× NA 0.45 Luc plan FLN or 40× NA 0.6 Luc Plan FL objectives. Images were acquired using a camera (DP70; Olympus) and DP manager software version 2.1.1.163 (Olympus). Time-lapse imaging of living cells used the Eclipse microscope and was performed with a temperature-controlled chamber (Solent Scientific) set to 37°C with continuous flow of 5% CO₂. Time-lapse two-photon imaging was performed at the lowest possible excitation levels. Images were captured every 10 min in single z planes with a monochromatic camera (CoolSNAP HQ; Photometrics) and a 6.45 × 6.45-µm pixel pitch (Photometrics) using MetaMorph software (Molecular Devices). After image acquisition, stacks of each stage position were assembled using MetaMorph software.

Statistical analysis

Statistical analysis of selected EC invasion, vasculogenesis, and regression data was performed using SPSS 11.0 software (SPSS, Inc.). Analysis of variance was used to compare means when analyzing more than two groups. The Tukey's post-hoc test was used to determine groups of similarity. Statistical significance was set at $P < 0.01$. Unpaired t tests were used when analyzing two groups within a single experiment.

Online supplemental material

Fig. S1 shows that EC invasion of 3D collagen matrices is markedly inhibited by ECs expressing TIMP-3 but not by ECs expressing TIMP-1 and that pericytes are an abundant source of TIMP-3. Fig. S2 shows that TIMP-3 stabilizes ECs undergoing EC tubular network formation or regression, whereas anti-α2-integrin–blocking antibodies cause the rapid collapse of EC tubular networks. Fig. S3 shows that TIMP-3 blocks further lumen development and network remodeling when added to preexisting EC tubular networks without causing the collapse of these structures. Fig. S4 shows that the suppression of membrane-associated metalloproteinases via siRNAs in ECs indicates a critical role for MT1-MMP in the S1P-mediated invasion of 3D collagen matrices. Fig. S5 shows that the suppression of membrane-associated metalloproteinases via siRNAs in ECs indicates a critical role for MT1-MMP, MT2-MMP, and ADAM-15 in the SDF-1α–mediated invasion of 3D collagen matrices. Video 1 is a time-lapse video of control EC tube morphogenesis in 3D collagen matrices. Video 2 is a time-lapse video of normal EC tube morphogenesis in the presence of TIMP-1 in 3D collagen matrices. Videos 3 and 4 are time-lapse videos of the blockade of EC tube morphogenesis by TIMP-2 and -3, respectively, in 3D collagen matrices. Video 5 is a time-lapse video of the blockade of EC tube morphogenesis by the MMP inhibitor GM6001 in 3D collagen matrices. Online supplemental material is available at http://www.jcb.org/cgi/content/full/jcb.200603176/DC1.

References

Anand-Apte, B., M.S. Pepper, E. Voest, R. Montesano, B. Olsen, G. Murphy, S.S. Apte, and B. Zetter. 1997. Inhibition of angiogenesis by tissue inhibitor of metalloproteinase-3. *Invest. Ophthalmol. Vis. Sci.* 38:817–823.

Baker, A.H., D.R. Edwards, and G. Murphy. 2002. Metalloproteinase inhibitors: biological actions and therapeutic opportunities. *J. Cell Sci.* 115:3719–3727.

Bayless, K.J., and G.E. Davis. 2003. Sphingosine-1-phosphate markedly induces matrix metalloproteinase and integrin-dependent human endothelial cell invasion and lumen formation in three-dimensional collagen and fibrin matrices. *Biochem. Biophys. Res. Commun.* 312:903–913.

Bell, S.E., A. Mavila, R. Salazar, K.J. Bayless, S. Kanagala, S.A. Maxwell, and G.E. Davis. 2001. Differential gene expression during capillary morphogenesis in 3D collagen matrices: regulated expression of genes involved in basement membrane matrix assembly, cell cycle progression, cellular differentiation and G-protein signaling. *J. Cell Sci.* 114:2755–2773.

Bohnsack, B.L., L. Lai, P. Dolle, and K.K. Hirschi. 2004. Signaling hierarchy downstream of retinoic acid that independently regulates vascular remodeling and endothelial cell proliferation. *Genes Dev.* 18:1345–1358.

Brew, K., D. Dinakarpandian, and H. Nagase. 2000. Tissue inhibitors of metalloproteinases: evolution, structure and function. *Biochim. Biophys. Acta*. 1477:267–283.

Campbell, R.E., O. Tour, A.E. Palmer, P.A. Steinbach, G.S. Baird, D.A. Zacharias, and R.Y. Tsien. 2002. A monomeric red fluorescent protein. *Proc. Natl. Acad. Sci. USA*. 99:7877–7882.

Carmeliet, P. 2005. Angiogenesis in life, disease and medicine. *Nature*. 438:932–936.

Ceradini, D.J., A.R. Kulkarni, M.J. Callaghan, O.M. Tepper, N. Bastidas, M.E. Kleinman, J.M. Capla, R.D. Galiano, J.P. Levine, and G.C. Gurtner. 2004. Progenitor cell trafficking is regulated by hypoxic gradients through HIF-1 induction of SDF-1. *Nat. Med.* 10:858–864.

Chun, T.H., F. Sabeh, I. Ota, H. Murphy, K.T. McDonagh, K. Holmbeck, H. Birkedal-Hansen, E.D. Allen, and S.J. Weiss. 2004. MT1-MMP-dependent neovessel formation within the confines of the three-dimensional extracellular matrix. *J. Cell Biol.* 167:757–767.

Curry, T.E., Jr., and K.G. Osteen. 2003. The matrix metalloproteinase system: changes, regulation, and impact throughout the ovarian and uterine reproductive cycle. *Endocr. Rev.* 24:428–465.

Davis, G.E., and D.R. Senger. 2005. Endothelial extracellular matrix: biosynthesis, remodeling, and functions during vascular morphogenesis and neovessel stabilization. *Circ. Res.* 97:1093–1107.

Davis, G.E., and W.B. Saunders. 2006. Molecular balance of capillary tube formation versus regression in wound repair: role of matrix metalloproteinases and their inhibitors. *J. Invest. Dermatol.* 126(Suppl.):44–56.

Davis, G.E., K.A. Pintar Allen, R. Salazar, and S.A. Maxwell. 2001. Matrix metalloproteinase-1 and -9 activation by plasmin regulates a novel endothelial cell-mediated mechanism of collagen gel contraction and capillary tube regression in three-dimensional collagen matrices. *J. Cell Sci.* 114:917–930.

Davis, G.E., K.J. Bayless, and A. Mavila. 2002. Molecular basis of endothelial cell morphogenesis in three-dimensional extracellular matrices. *Anat. Rec.* 268:252–275.

Green, K.A., and L.R. Lund. 2005. ECM degrading proteases and tissue remodelling in the mammary gland. *Bioessays*. 27:894–903.

Hellstrom, M., M. Kalen, P. Lindahl, A. Abramsson, and C. Betsholtz. 1999. Role of PDGF-B and PDGFR-beta in recruitment of vascular smooth muscle cells and pericytes during embryonic blood vessel formation in the mouse. *Development*. 126:3047–3055.

Hellstrom, M., H. Gerhardt, M. Kalen, X. Li, U. Eriksson, H. Wolburg, and C. Betsholtz. 2001. Lack of pericytes leads to endothelial hyperplasia and abnormal vascular morphogenesis. *J. Cell Biol.* 153:543–553.

Hirschi, K.K., S.A. Rohovsky, and P.A. D'Amore. 1998. PDGF, TGF-β, and heterotypic cell-cell interactions mediate endothelial cell-induced recruitment of 10T1/2 cells and their differentiation to a smooth muscle fate. *J. Cell Biol.* 141:805–814.

Horiuchi, K., G. Weskamp, L. Lum, H.P. Hammes, H. Cai, T.A. Brodie, T. Ludwig, R. Chiusaroli, R. Baron, K.T. Preissner, et al. 2003. Potential role for ADAM15 in pathological neovascularization in mice. *Mol. Cell. Biol.* 23:5614–5624.

Hotary, K., E. Allen, A. Punturieri, I. Yana, and S.J. Weiss. 2000. Regulation of cell invasion and morphogenesis in a three-dimensional type I collagen matrix by membrane-type matrix metalloproteinases 1, 2, and 3. *J. Cell Biol.* 149:1309–1323.

Hotary, K.B., I. Yana, F. Sabeh, X.Y. Li, K. Holmbeck, H. Birkedal-Hansen, E.D. Allen, N. Hiraoka, and S.J. Weiss. 2002. Matrix metalloproteinases (MMPs) regulate fibrin-invasive activity via MT1-MMP-dependent and -independent processes. *J. Exp. Med.* 195:295–308.

Jain, R.K. 2003. Molecular regulation of vessel maturation. *Nat. Med.* 9:685–693.

Jain, R.K. 2005. Normalization of tumor vasculature: an emerging concept in antiangiogenic therapy. *Science*. 307:58–62.

Kheradmand, F., and Z. Werb. 2002. Shedding light on sheddases: role in growth and development. *Bioessays*. 24:8–12.

Kryczek, I., A. Lange, P. Mottram, X. Alvarez, P. Cheng, M. Hogan, L. Moons, S. Wei, L. Zou, V. Machelon, et al. 2005. CXCL12 and vascular endothelial growth factor synergistically induce neoangiogenesis in human ovarian cancers. *Cancer Res.* 65:465–472.

Lafleur, M.A., P.A. Forsyth, S.J. Atkinson, G. Murphy, and D.R. Edwards. 2001. Perivascular cells regulate endothelial membrane type-1 matrix metalloproteinase activity. *Biochem. Biophys. Res. Commun.* 282:463–473.

Lafleur, M.A., M.M. Handsley, V. Knauper, G. Murphy, and D.R. Edwards. 2002. Endothelial tubulogenesis within fibrin gels specifically requires the activity of membrane-type-matrix metalloproteinases (MT-MMPs). *J. Cell Sci.* 115:3427–3438.

Lai, L., B.L. Bohnsack, K. Niederreither, and K.K. Hirschi. 2003. Retinoic acid regulates endothelial cell proliferation during vasculogenesis. *Development*. 130:6465–6474.

Langton, K.P., M.D. Barker, and N. McKie. 1998. Localization of the functional domains of human tissue inhibitor of metalloproteinases-3 and the effects of a Sorsby's fundus dystrophy mutation. *J. Biol. Chem.* 273:16778–16781.

Lindahl, P., B.R. Johansson, P. Leveen, and C. Betsholtz. 1997. Pericyte loss and microaneurysm formation in PDGF-B-deficient mice. *Science*. 277:242–245.

Nagase, H., and J.F. Woessner Jr. 1999. Matrix metalloproteinases. *J. Biol. Chem.* 274:21491–21494.

Nayak, R.C., A.B. Berman, K.L. George, G.S. Eisenbarth, and G.L. King. 1988. A monoclonal antibody (3G5)-defined ganglioside antigen is expressed on the cell surface of microvascular pericytes. *J. Exp. Med.* 167:1003–1015.

Oh, J., R. Takahashi, S. Kondo, A. Mizoguchi, E. Adachi, R.M. Sasahara, S. Nishimura, Y. Imamura, H. Kitayama, D.B. Alexander, et al. 2001. The membrane-anchored MMP inhibitor RECK is a key regulator of extracellular matrix integrity and angiogenesis. *Cell*. 107:789–800.

Orlidge, A., and P.A. D'Amore. 1987. Inhibition of capillary endothelial cell growth by pericytes and smooth muscle cells. *J. Cell Biol.* 105:1455–1462.

Pepper, M.S. 2001. Role of the matrix metalloproteinase and plasminogen activator-plasmin systems in angiogenesis. *Arterioscler. Thromb. Vasc. Biol.* 21:1104–1117.

Qi, J.H., Q. Ebrahem, N. Moore, G. Murphy, L. Claesson-Welsh, M. Bond, A. Baker, and B. Anand-Apte. 2003. A novel function for tissue inhibitor of metalloproteinases-3 (TIMP3): inhibition of angiogenesis by blockage of VEGF binding to VEGF receptor-2. *Nat. Med.* 9:407–415.

Saunders, W.B., K.J. Bayless, and G.E. Davis. 2005. MMP-1 activation by serine proteases and MMP-10 induces human capillary tubular network collapse and regression in 3D collagen matrices. *J. Cell Sci.* 118:2325–2340.

Seo, D.W., H. Li, L. Guedez, P.T. Wingfield, T. Diaz, R. Salloum, B.Y. Wei, and W.G. Stetler-Stevenson. 2003. TIMP-2 mediated inhibition of angiogenesis: an MMP-independent mechanism. *Cell*. 114:171–180.

Spurbeck, W.W., C.Y. Ng, T.S. Strom, E.F. Vanin, and A.M. Davidoff. 2002. Enforced expression of tissue inhibitor of matrix metalloproteinase-3 affects functional capillary morphogenesis and inhibits tumor growth in a murine tumor model. *Blood*. 100:3361–3368.

Stetler-Stevenson, W.G., and D.W. Seo. 2005. TIMP-2: an endogenous inhibitor of angiogenesis. *Trends Mol. Med.* 11:97–103.

von Tell, D., A. Armulik, and C. Betsholtz. 2006. Pericytes and vascular stability. *Exp. Cell Res.* 312:623–629.

Wild, A., A. Ramaswamy, P. Langer, I. Celik, V. Fendrich, B. Chaloupka, B. Simon, and D.K. Bartsch. 2003. Frequent methylation-associated silencing of the tissue inhibitor of metalloproteinase-3 gene in pancreatic endocrine tumors. *J. Clin. Endocrinol. Metab.* 88:1367–1373.